Journal for ImmunoTherapy of Cancer

# Nemvaleukin alfa, a novel engineered IL-2 fusion protein, drives antitumor immunity and inhibits tumor growth in small cell lung cancer

Yuanwang Pan,[1] Yuan Hao,[2] Han Han,[1] Ting Chen,[1] Hailin Ding,[1] Kristen E Labbe,[1] Elaine Shum,[1] Kayla Guidry,[1] Hai Hu,[1] Fiona Sherman,[1] Ke Geng,[1] Janaye Stephens,[1] Alison Chafitz,[1] Sittinon Tang,[1] Hsin-Yi Huang,[1] Chengwei Peng,[1] Christina Almonte,[1] Jared E Lopes,[3] Heather C Losey,[3] Raymond J Winquist,[3] Vamsidhar Velcheti,[1] Hua Zhang ,[1] Kwok-Kin Wong[1]

**To cite:** Pan Y, Hao Y, Han H, *et al*. Nemvaleukin alfa, a novel engineered IL-2 fusion protein, drives antitumor immunity and inhibits tumor growth in small cell lung cancer. *Journal for ImmunoTherapy of Cancer* 2022;**10**:e004913. doi:10.1136/jitc-2022-004913

► Additional supplemental material is published online only. To view, please visit the journal online (http://dx.doi.org/10.1136/jitc-2022-004913).

YP, YH and HH contributed equally.

Accepted 28 July 2022



For numbered affiliations see end of article.

**Correspondence to**
Dr Hua Zhang;
hua.zhang@nyulangone.org

Dr Kwok-Kin Wong;
kwok-kin.wong@nyulangone.org

## ABSTRACT

**Background** Small cell lung cancer (SCLC) is a deadly disease with a 5-year survival of less than 7%. The addition of immunotherapy to chemotherapy was recently approved as first-line treatment; however, the improved clinical benefit is modest, highlighting an urgent need for new treatment strategies. Nemvaleukin alfa, a novel engineered interleukin-2 fusion protein currently in phase I–III studies, is designed to selectively expand cytotoxic natural killer (NK) cells and $CD8^+$ T cells. Here, using a novel SCLC murine model, we investigated the effects of a mouse version of nemvaleukin (mNemvaleukin) on tumor growth and antitumor immunity.

**Methods** A novel *Rb1*$^{-/-}$*p53*$^{-/-}$*p130*$^{-/-}$ SCLC model that mimics human disease was generated. After confirming tumor burden by MRI, mice were randomized into four treatment groups: vehicle, mNemvaleukin alone, chemotherapy (cisplatin+etoposide) alone, or the combination of mNemvaleukin and chemotherapy. Tumor growth was measured by MRI and survival was recorded. Tumor-infiltrating lymphocytes and peripheral blood immune cells were analyzed by flow cytometry. Cytokine and chemokine secretion were quantified and transcriptomic analysis was performed to characterize the immune gene signatures.

**Results** mNemvaleukin significantly inhibited SCLC tumor growth, which was further enhanced by the addition of chemotherapy. Combining mNemvaleukin with chemotherapy provided the most significant survival benefit. Profiling of tumor-infiltrating lymphocytes revealed mNemvaleukin expanded the total number of tumor-infiltrating NK and $CD8^+$ T cells. Furthermore, mNemvaleukin increased the frequencies of activated and proliferating NK and $CD8^+$ T cells in tumors. Similar immune alterations were observed in the peripheral blood of mNemvaleukin-treated mice. Of note, combining mNemvaleukin with chemotherapy had the strongest effects in activating effector and cytotoxic $CD8^+$ T cells. mNemvaleukin alone, and in combination with chemotherapy, promoted proinflammatory cytokine and chemokine production, which was further confirmed by transcriptomic analysis.

**Conclusions** mNemvaleukin, a novel cytokine-based immunotherapy, significantly inhibited murine SCLC tumor growth and prolonged survival, which was further enhanced by the addition of chemotherapy. mNemvaleukin alone, and in combination with chemotherapy, drove a strong antitumor immune program elicited by cytotoxic immune cells. Our findings support the evaluation of nemvaleukin alone or in combination with chemotherapy in clinical trials for the treatment of SCLC.

### WHAT IS ALREADY KNOWN ON THIS TOPIC

⇒ Small cell lung cancer (SCLC) is an aggressive type of cancer with extremely poor prognosis. Combining immunotherapy with chemotherapy is approved as the first-line treatment for SCLC, but the improved clinical benefit is modest. Therefore, the identification of new treatment paradigms is urgently needed.

### WHAT THIS STUDY ADDS

⇒ The mouse version of nemvaleukin (mNemvaleukin), a novel engineered interleukin-2 fusion protein, inhibits SCLC tumor growth and combining mNemvaleukin with chemotherapy further improves response and survival.

⇒ mNemvaleukin alone and in combination expand tumor-infiltrating cytotoxic natural killer cells and $CD8^+$ T cells. mNemvaleukin triggers robust antitumor immune response signaling, which is enhanced by the addition of chemotherapy.

### HOW THIS STUDY MIGHT AFFECT RESEARCH, PRACTICE OR POLICY

⇒ Our findings support the evaluation of nemvaleukin alone or in combination with chemotherapy in clinical trials for the treatment of SCLC.

## BACKGROUND

Small cell lung cancer (SCLC) is a high-grade neuroendocrine carcinoma with an extremely poor prognosis, accounting for

about 15% of all lung cancers.[1 2] It most commonly arises in heavy smokers and is characterized by rapid growth and early metastasis; two-thirds of patients have distant metastatic disease at initial diagnosis.[2–4] Genome sequencing studies have revealed a high rate of mutations in SCLC tumors compared with other forms of cancer[5]; however, these efforts have yet to identify driver mutations amenable to therapeutic intervention. This stands in stark contrast to non-small cell lung cancer (NSCLC), in which some patients harbor defined activating mutations in kinase signaling pathways, such as epidermal growth factor receptor (EGFR), show predictably strong clinical responses to targeted kinase inhibition. Instead, inactivating mutations of the tumor suppressor genes *TP53* and *RB1* are found in nearly all SCLC tumors along with mutations in a wide range of epigenetic modulators.[6–8] Patients with SCLC often initially respond to chemotherapy, but tumors typically relapse within 6–12 months, resulting in a 5-year survival rate of less than 7%.[1]

Immune checkpoint blockade (ICB), which includes antibodies that block inhibitory immune-checkpoint proteins such as programmed cell death protein 1 (PD-1), its ligand (PD-L1), or cytotoxic T-lymphocyte-associated protein 4, has emerged as the standard of care in the management of various cancers.[9] The high tumor mutation burden (TMB) in SCLC has offered a strong rationale for examining the effects of ICB in this tumor type, but the overall response rate of patients with SCLC to ICB alone is relatively low.[6 10–12] Recently, the addition of immunotherapy (such as anti-PD-L1 therapy) to chemotherapy was approved in the first-line treatment of adult patients with extensive-stage small cell lung cancer (ES-SCLC); however, the improved clinical benefit is modest with an added median overall survival (OS) of approximately 2 months.[13 14] The identification of new targets and treatment paradigms for this malignant disease is urgently needed.

The tumor microenvironment (TME) of SCLC is characterized by poor immune cell infiltration in comparison to that of NSCLC. Immunohistochemistry (IHC) staining of patients' tissues revealed an immune desert phenotype associated with low numbers of tumor-infiltrating lymphocytes including $CD45^+$, $CD3^+$, $CD8^+$, and $CD20^+$ cells.[15 16] Encouragingly, approaches that enhance immune cell infiltration and target cytotoxic effector populations have recently been explored and showed promise in preclinical models.[17 18] For example, activation of natural killer (NK) cells through augmentation of interleukin (IL)-15 or transforming growth factor-β signaling pathways ameliorated SCLC metastases.[17]

IL-2 plays an essential role in regulating immune homeostasis, activating several key lymphocyte subsets with either immunostimulatory or suppressive functions such as NK cells, effector $CD4^+$ and $CD8^+$ T cells, as well as regulatory T cells ($T_{regs}$).[19 20] Therefore, it has been pursued as a treatment option to activate the antitumor immune response. Indeed, recombinant human interleukin-2 (rhIL-2) has offered significant clinical benefit with durable responses and is approved for the treatment of metastatic melanoma and renal cell carcinoma,[21–23] but its use is considerably limited due to the associated side effects. An additional limiting factor of rhIL-2 utility is that it favorably activates and induces the expansion of immunosuppressive $CD4^+$ $T_{regs}$, which directly inhibit antitumor immunity.[19 24] This differential activation of $T_{regs}$ over NK and effector T cells results from the distinct interactions between IL-2 and two versions of the IL-2 receptor (IL-2R) complexes with differing affinities expressed on these immune cell populations. Low concentrations of IL-2 relay signaling through the high-affinity IL-2R composed of IL-2Rα, IL-2Rβ, and common γ chain ($\gamma_c$), which are preferentially expressed on $T_{regs}$. Higher concentrations of IL-2 are required to activate signaling through the intermediate-affinity IL-2R, composed of IL-2Rβ and $\gamma_c$, which are expressed on memory $CD8^+$ T cells and NK cells. We have recently characterized nemvaleukin alfa ('nemvaleukin', previously known as ALKS 4230), a fusion protein of circularly permuted IL-2 to the extracellular domain of IL-2Rα, designed to interact with the intermediate-affinity IL-2R and not the high-affinity IL-2R to selectively activate effector lymphocytes.[25] In primary human cells from healthy donors and patients with advanced cancer, nemvaleukin resulted in superior activation and expansion of NK cells and memory $CD8^+$ T cells with less expansion of $T_{regs}$ relative to rhIL-2 in vitro.[25] Likewise, nemvaleukin led to an increase of NK cells and memory $CD8^+$ T cells at doses that did not expand or activate $T_{regs}$ in vivo; it exhibited superior antitumor efficacy in the mouse B16F10 lung tumor model.[25] Furthermore, preferential expansion of $CD8^+$ T cells and $CD56^+$ NK cells and minimal expansion of immunosuppressive $T_{regs}$ were observed in cynomolgus monkeys.[26] These data support strong systemic antitumor immunity elicited by treatment with nemvaleukin, which is currently under clinical investigation as monotherapy and in combination with ICB in patients with advanced solid tumors (including NCT03861793, NCT02799095, NCT04830124, and NCT05092360).

In this study, using a novel immunocompetent orthotopic mouse SCLC model, we examined the effects of mouse version of nemvaleukin (mNemvaleukin) alone and in combination with standard chemotherapy in tumor response and antitumor immunity elicited through NK and effector T cells. Our findings highlight that nemvaleukin has the potential to be an effective cancer immunotherapy in SCLC and further support its development in clinical trials.

## MATERIALS AND METHODS

### Animal model

The SCLC orthotopic model harboring conditional mutant *Rb*, *p53*, and *p130* (RPP) has been described previously.[27] Briefly, ultrasound-guided transthoracic injection was performed using 200,000 RPP cells in 20 µL phosphate-buffered saline (PBS) into C57BL/6J mice

of 6–8 weeks old (Jackson Laboratory, stock number 000664).

### In vivo treatment studies

For treatment studies, mice were evaluated by MRI (Preclinical Imaging Core, NYULH) to quantify lung tumor burden before randomization and after drug treatment for efficacy evaluation. Mice were treated with either vehicle (PBS), chemotherapy (cisplatin 5 mg/kg intraperitoneal once a week, q.w.+etoposide 10 mg/kg intraperitoneal 3 times a week, t.i.w.), mNemvaleukin (subcutaneous) every 4 days at 6 mg/kg or the combination of chemotherapy with mNemvaleukin for 3 weeks.

### MRI quantification

Animals were anesthetized with isoflurane to perform MRI of the lung field using BioSpec USR70/30 horizontal bore system (Bruker) to scan 16 consecutive sections. Tumor volumes within the whole lung were quantified using three-dimensional slicer software to reconstruct MRI volumetric measurements as described previously. Acquisition of the MRI signal was adapted according to cardiac and respiratory cycles to minimize motion effects during imaging.

### Tumor-infiltrating immune cell profiling

Mice were humanely euthanized, and mouse lungs were perfused using sterile PBS through heart perfusion from the left ventricle after bronchoalveolar lavage fluid (BALF) collection. The whole lung was cut and minced into small pieces followed by digestion in collagenase D (Sigma) and DNase I (Sigma) in Hank's balanced salt solution at 37°C for 30 min. After incubation, the digested tissue was subjected to a 70 µm cell strainer (ThermoFisher Scientific) to obtain single-cell suspensions. Separated cells were treated with 1×RBC lysis buffer (BioLegend) to lyse red blood cells. Live cells were determined by LIVE/DEAD fixable aqua dead cell stain kit (Molecular Probes). The cell pellets were resuspended in PBS with 2% FBS for flow cytometry analysis. Cells were stained with cell surface markers as indicated followed by fixation/permeabilization (eBioscience). Cells were imaged on BD LSRFortessa (BD Biosciences) and analyzed using FlowJo software (Tree Star).

### Peripheral blood mononuclear cell profiling

After mice were humanely euthanized, peripheral blood was collected from the heart (intracardiac blood collection). The peripheral blood was then put into Eppendorf tubes containing 15 µL sodium citrate buffer, followed by fixation in eBioscience 1-step Fix/Lyse Solution for 20 min at room temperature. After washing in flow cytometry buffer (PBS with 2% FBS) two times. Cells were stained with cell surface markers as indicated followed by fixation/permeabilization (eBioscience). Cells were imaged on BD LSRFortessa (BD Biosciences) and analyzed using FlowJo software (Tree Star).

### Luminex analysis of murine BALF

Mouse lung BALF was performed by intratracheal injection of 2 mL of sterile PBS followed by collection by aspiration. interferon gamma (IFN-γ), CXCL9, and CXCL10 levels were measured using mouse Cytokine/Chemokine 32-plex Assay (MILLIPLEX, Millipore) on Luminex SD system (Luminex). Concentrations (pg/mL) of each protein were derived from five-parameter curve fitting models according to the manufacturer's instructions.

### RNA extraction and bulk-RNA sequencing analysis

Tumor nodules (n=2 per treatment group) were harvested and stored in RNAlater Stabilization Solution (ThermoFisher, AM7020). Tumor nodules were then subjected to total RNA extraction using RNeasy Plus Mini Kit (QIAGEN, cat# 74136) according to the manufacturer's instructions. Read qualities were evaluated using FASTQC (Babraham Institute) and mapping to GRCm38 (GENCODE M25) reference genome using STAR program[28] with default parameters. Read counts, transcripts per million (TPM) and reads per kilobase of transcript per million reads mapped (FPKM) were calculated using RSEM program.[29] Identification of differentially expressed genes was performed using DESeq2 in R/Bioconductor (R V.4.0.4). Genes with false discovery rate lower than 0.05 were considered significantly differentially expressed.

All plots were generated using customized R scripts. Pathway enrichment analysis was performed on all genes ranked from high to low DESeq2 estimated fold change using the GSEAPreRanked function with enrichment statistic classic and 1000 permutations using gene set enrichment analysis (GSEA) program.[30] Gene sets (hallmark and C7 'immunologic signature gene sets' (V.7.1)) were downloaded from MsigDB.[31] Differential expression genes involved in top enriched pathways were selected to generate heatmaps using pheatmap R function with default hierarchical clustering method for gene orders. For large pathways, genes were truncated based on absolute log2FC values for visualization purpose. Additionally, a customized gene set associated with antigen presentation (*B2m*), interferon signaling (*Irf4*, *Irf7*, and *Irf8*), cytotoxic granzymes (*Gzma*, *Gzma*, *Gzmc*, *Gzmd*, and *Gzme*), NK cells (*Nkg7* and *Ncr1*), and antitumor cytokines/chemokines (*Tnf*, *Ifng*, *Cxcl9*, and *Cxcl10*) were established and heatmap was generated based on their normalized expression values.

### Immunohistochemistry

Lungs were perfused with 10% formalin, stored in fixative overnight, processed through graded ethanols, xylene, and into paraffin in a Leica Peloris automated processor. Five-micron paraffin-embedded sections were either stained with H&E or immunostained on a Leica BondRX autostainer, according to the manufacturers' instructions. In brief, sections underwent epitope retrieval for 20 min at 100°C with Leica Biosystems ER2 solution (pH9 and AR9640) followed by incubation with either anti-CD3

(CST, 78588S) diluted 1:1000, anti-CD8 (CST, 98941S) diluted 1:400, NKp46 (R&D, AF2225) diluted 1:75. Anti-CD3 or CD8 were detected using BOND Polymer Refine Detection System (Leica, DS9800). For NKp46 detection, the anti-rabbit HRP polymer in the detection system was replaced with Goat-on-Rodent HRP Polymer (Biocare GHP516 H). Sections were scanned on either a Leica AT2 or Hamamatsu Nanozoomer HT whole slide scanner.

### Single-cell RNA-seq experiment protocol

Single-cell RNA-seq experiment was carried out as previously described.[27] Single-cell suspensions were obtained as described in the Tumor-infiltrating immune cell profiling section and were sorted using 4′,6-diamidino-2-phenylindole (DAPI) staining. Cells were then resuspended into single cells at a concentration of $1\times10^6$ per mL in 1× PBS with 0.04% bovine serum albumin (BSA) for 10× genomics processing. Cell suspensions were loaded onto a 10× Genomics Chromium instrument to generate single-cell gel beads in emulsion. Approximately 5000–10,000 cells were loaded per channel. Single-cell RNA sequencing (scRNA-seq) libraries were prepared using the following Single Cell 3′ Reagent Kits: Chromium Single Cell 3′ Library & Gel Bead Kit v2 (PN-120237), Single Cell 3′ Chip Kit v2 (PN-120236) and i7 Multiplex Kit (PN-120262) (10× Genomics, Pleasanton, California, USA) following the Single Cell 3′ Reagent Kits V.2 User Guide (manual part #CG00052 Rev A). Libraries were run on an Illumina HiSeq 4000 system (SY-401–4001, Illumina) as 2×150 paired-end reads, one full lane per sample, for approximately >90% sequencing saturation.

### Single-cell RNA-seq analysis

Cell Ranger Single-Cell Software Suite was used to perform sample demultiplexing, mapping (GRCm38 genome reference), barcode processing, and gene expression quantification. Filtered gene-barcode matrices that contained only barcodes with unique molecular identifier counts that passed the threshold for cell detection were imported into R as a Seurat[32] (V.4.1.0) object for further analysis. Cells with less than 200 genes detected or greater than 10% mitochondrial RNA content were deemed as low quality and excluded from the analysis. RNA counts were normalized using Seurat::SCTransform function with regressions of cell cycle score and ribosomal and mitochondrial percentages for each sample. Multiple samples were integrated using Seurat standard scRNSeq integration workflow with 3000 anchor genes. A shared nearest neighbor graph was then built based on the first 40 principal components followed by identification of cell clusters using Leiden algorithm. The same principal components were used to generate the uniform manifold approximation and projection (UMAP) projection. Cell types were manually annotated based on canonical cell type markers and differential expressed genes of each cluster identified using Seurat::FindAllMarkers function with a logistic regression model.

### Statistical analysis

Statistical analyses were performed using GraphPad Prism V.9 software and statistical significance was determined by $p<0.05$. Data are presented as mean with SEM unless otherwise specified. Statistical comparisons were performed using unpaired Student t-test for two-tailed p values unless otherwise specified (*p<0.05, **p<0.01, ***p<0.001, ****p<0.0001).

## RESULTS

### mNemvaleukin inhibits SCLC tumor growth and enhances tumor response to chemotherapy

We previously characterized nemvaleukin, a fusion protein of circularly permuted IL-2 to the extracellular domain of IL-2Rα, which can selectively expand tumor-killing NK cells and $CD8^+$ T cells (figure 1A). Because enhancing cytotoxic effector immune cell infiltration is a promising treatment approach for SCLC, we hypothesize that nemvaleukin treatment could be effective in SCLC. We used mNemvaleukin in the study, and used a novel immunocompetent orthotopic $Rb1^{-/-}p53^{-/-}p130^{-/-}$ (RPP) SCLC model that closely mimics human disease (figure 1B). These syngeneic SCLC models are ideal for therapeutic studies in immune-oncology research, because they have a shorter and consistent latency, and a highly similar frequency of different immune infiltrating populations, in comparison to the conventional genetically engineered mouse models.[27]

We sought to evaluate whether mNemvaleukin alone and in combination with standard-of-care chemotherapy would inhibit tumor growth in the RPP SCLC model. Under ultrasound guidance, we performed the transthoracic injection of RPP cells into the C57BL/6J (B6) mouse lung and monitored the tumor growth by MRI. After confirming tumor burden, mice were randomized into one of four groups: vehicle, mNemvaleukin alone (every 4 days at 6 mg/kg for 3 weeks), chemotherapy alone (cisplatin 5 mg/kg+etoposide 10 mg/kg), and mNemvaleukin combined with chemotherapy groups (figure 1C). Of note, no significant decrease in body weight as a measure of toxicity was detected with mNemvaleukin monotherapy or in the combination treatment group (online supplemental figure 1A). The baseline tumor burden was comparable between the vehicle and drug treatment groups (figure 1D). All vehicle-treated mice demonstrated aggressive disease, with tumor volumes doubling after a 3-week period (figure 1E–G). mNemvaleukin-treated mice had a significant antitumor response with a slower tumor growth (figure 1E–G).

Similar to mNemvaleukin monotherapy, chemotherapy alone significantly delayed tumor growth (figure 1E–G and online supplemental figure 1B,C), and mice in the combined chemotherapy and mNemvaleukin treatment regimen (combo) had the best response (figure 1E–G and online supplemental figure 1B,C). Most importantly, combining mNemvaleukin with chemotherapy increased the OS of tumor-bearing mice in comparison to that

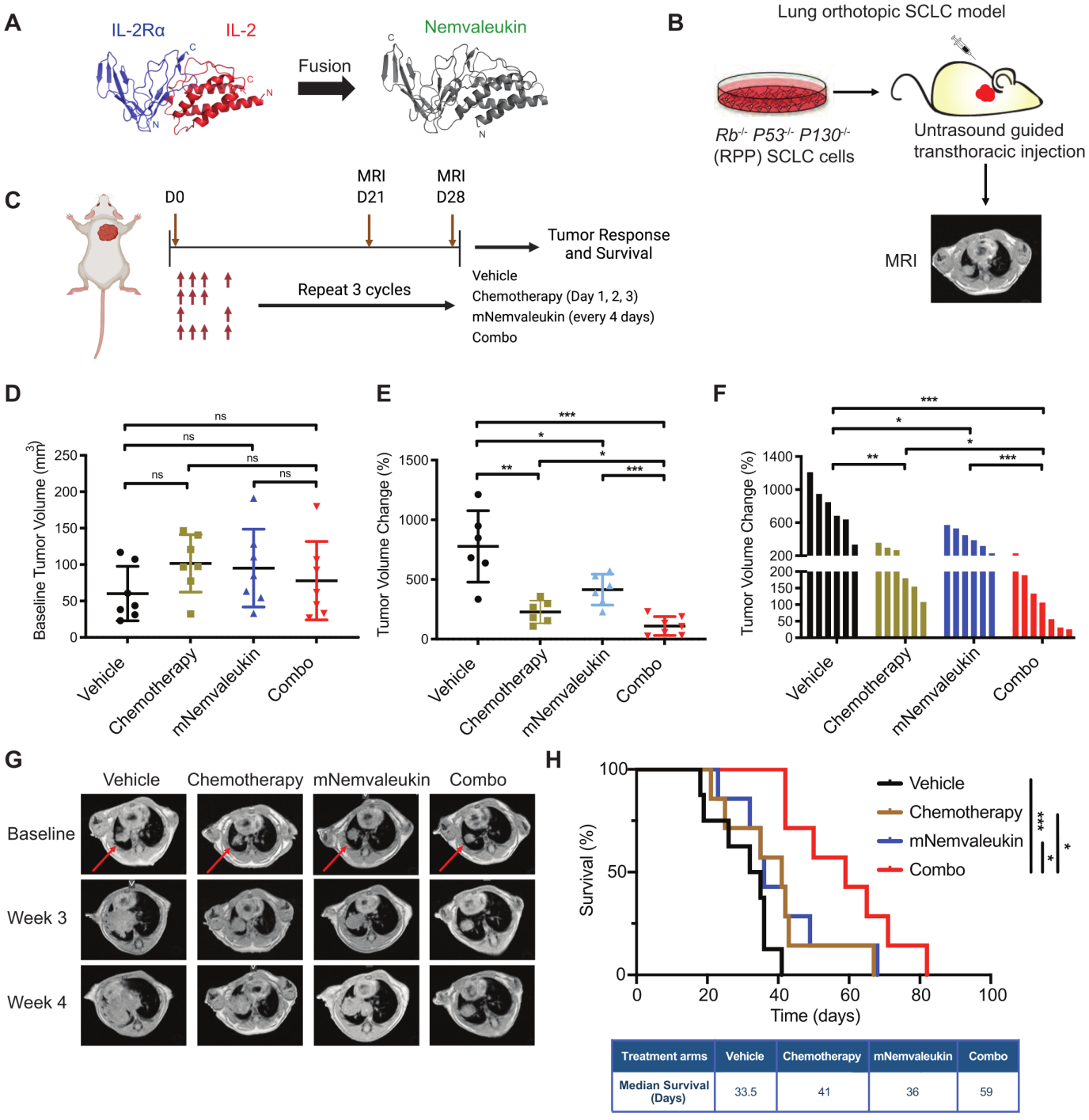


| Treatment arms | Vehicle | Chemotherapy | mNemvaleukin | Combo |
|---|---|---|---|---|
| Median Survival (Days) | 33.5 | 41 | 36 | 59 |

**Figure 1** mNemvaleukin inhibits SCLC tumor growth and enhances tumor response to chemotherapy. (A) Visualization of spatial distance between unfused IL-2Rα and IL-2 (left, with native N-termini and C-termini labeled) and the resulting fused nemvaleukin alfa (right). (B) Schematic illustration of SCLC model. *Rb1*$^{-/-}$*p53*$^{-/-}$*p130*$^{-/-}$ (RPP) SCLC cells were cultured and expanded in vitro, and subsequently, ultrasound-guided transthoracic injection of RPP cells was performed to generate the orthotopic lung tumor. Tumor volume was monitored by MRI weekly. (C) Schematic showing in vivo dosing schedule. Mice were treated with mNemvaleukin alone (every 4 days at 6 mg/kg for 3 weeks) or in combination with standard chemotherapy (cisplatin 5 mg/kg q.w.+etoposide 10 mg/kg t.i.w. for 3 weeks) for three cycles. Tumor growth was measured by MRI and survival was recorded. (D) Baseline tumor burden was quantified and presented. Dot plot (E) and waterfall plot (F) of changes in tumor volume were calculated 4 weeks after treatment initiation. Two independent cohorts of experiments were performed: vehicle (n=6), chemotherapy (n=6), mNemvaleukin (n=6), and combo (n=7). (G) Representative MR images of tumor baseline, 3 weeks and 4 weeks after treatment initiation. The red arrowheads indicate the lung tumors. (H) Kaplan-Meier survival curve for the RPP SCLC model after indicated treatment. Two independent cohorts of experiments were performed: vehicle (n=8), chemotherapy (n=7), mNemvaleukin (n=7), and combo (n=7). Data shown as means±SEM. *P<0.05, **P<0.01, ***P<0.001. IL, interleukin; mNemvaleukin, mouse version of nemvaleukin; ns, not significant (unpaired two-tailed t test); RPP, *Rb, p53, and p130*; SCLC, small cell lung cancer.

of the vehicle, chemotherapy or mNemvaleukin alone (figure 1H). Compared with the vehicle, combination treatment led to almost a twofold increase in OS, with an added median survival benefit of 25.5 days.

In summary, our in vivo therapeutic study suggests that mNemvaleukin significantly delayed tumor growth and prolonged survival, and furthermore, combining mNemvaleukin with chemotherapy was superior to mNemvaleukin or chemotherapy alone and achieved the most significant antitumor efficacy and survival benefit.

### mNemvaleukin alone and combination treatments expand tumor-infiltrating NK cells in SCLC

Our previous studies indicated that nemvaleukin can expand NK cells and effector $CD8^+$ T cells in vitro and in vivo in non-tumor bearing mice.[25] To investigate the impact on the tumor-infiltrating lymphocytes by mNemvaleukin in SCLC, we treated tumor-bearing mice for 7 days and harvested lung tumors for immune profiling by multicolor flow cytometry (figure 2A and online supplemental figure 2A). Although there was no significant change of the frequency of total $CD45^+$ cell infiltrates after single agent or combination treatment when compared with the control tumors, a clear increase was observed (online supplemental figure 2B). Profiling of NK cells demonstrated significant increases in the frequency and activity with mNemvaleukin alone and combination treatments. Specifically, mNemvaleukin alone and combination treatments significantly expanded the total number of tumor-associated NK cells, compared with the vehicle-treated mice (figure 2B,C). In contrast, chemotherapy failed to affect NK-cell infiltration in the tumor. To explore the functional activity of NK cells, we next analyzed the expression of the activation marker CD69 and the proliferation marker Ki-67 on NK cells. Both mNemvaleukin monotherapy and combination therapy led to a much higher frequency of $CD69^+$ NK cells and induced an elevation of Ki-$67^+$ NK cells (figure 2D,E). To further assess the NK-cell infiltration in the tumor, we performed IHC staining of NKp46, a selective marker of NK cells, in tumor-bearing lungs after 7 days of treatment (figure 2F). Consistent with the immune profiling analysis, mNemvaleukin alone and combination treatments increased NK- cell infiltration in the tumors. Collectively, mNemvaleukin treatment alone significantly expanded the total number of NK cells and enhanced the activation and proliferation NK cells in SCLC, which was also observed with combination treatments.

### mNemvaleukin alone and combination treatments expand tumor-infiltrating effector and cytotoxic $CD8^+$ T cells in SCLC

To assess whether mNemvaleukin affects the tumor-infiltrating T cells in SCLC, we analyzed the frequency and functionality of T cells after 7 days of treatment. Similar to the effects on NK cells, mNemvaleukin alone and combination treatments both led to an increase in the frequency of $CD3^+$ T cells (online supplemental figure 2C). Particularly, an increase in the percentage of tumor-infiltrating $CD8^+$ T cells was detected in the mNemvaleukin alone and combination treatment groups, but not in the chemotherapy group (figure 3A,B). To further examine the functional activity of $CD8^+$ T cells, we analyzed the expression of CD69, Ki-67, and an effector T-cell marker, CD44. mNemvaleukin and combination treatments significantly increased the frequency of $CD69^+CD8^+$ T cells, indicating increased infiltration of activated $CD8^+$ T cells (figure 3C). mNemvaleukin monotherapy and combination treatments also led to a marked increase of tumor-infiltrating $CD8^+$ T cells expressing Ki-67 and CD44 (figure 3D,E). We next assessed the activity of cytotoxic $CD8^+$ T cells by staining for granzyme B (GZMB), a cytotoxic granule protein secreted by $CD8^+$ T cells. mNemvaleukin and combination treatments resulted in the highest level of GZMB expression in $CD8^+$ T cells (figure 3F). A significantly higher $CD8^+/T_{regs}$ ratio was also observed following mNemvaleukin and combination treatments (figure 3G).

To further confirm the increased levels of tumor-infiltrating T cells, we performed IHC staining for the T-cell markers CD3 and CD8 in tumor-bearing lungs after 7 days of treatment. Consistently, mNemvaleukin and combination treatments, but not chemotherapy alone, considerably increased the $CD3^+$ and $CD8^+$ expressing T cells in the tumors (figure 3H,I). Collectively, mNemvaleukin provokes robust antitumor immunity involving a significant expansion of activated and effector $CD8^+$ T cells. These indices of antitumor immunity were also observed when combining mNemvaleukin with chemotherapy.

### mNemvaleukin increases proinflammatory cytokines/chemokines and expands activated NK cells and $CD8^+$ T cells in the peripheral blood

Proinflammatory cytokines and chemokines play an essential role in regulating antitumor immunity. For instance, cytokines and chemokines, such as IFN-γ, CXCL9, and CXCL10, are involved in modulating T-cell activation and recruitment. To directly examine the in vivo secretion of these cytokines and chemokines in the TME, we collected BALF from the mouse lung after 7 days of treatment for Luminex analysis (figure 4A). mNemvaleukin treatment promoted a pronounced increase of IFN-γ, CXCL9, and CXCL10 (figure 4B–D). Of note, combining mNemvaleukin with chemotherapy resulted in the most significant increase of the proinflammatory cytokine IFN-γ (figure 4B), likely contributing to its superior efficacy and greater survival benefit.

To characterize the systemic effects of mNemvaleukin on immune cells, we collected the peripheral blood from treated mice for immune profiling by flow cytometry. Consistent with the effects on tumor-infiltrating lymphocytes, mNemvaleukin alone and combination treatments also expanded $CD49b^+$ NK cells with expansion in the combination cohort but was not statistically significant (figure 4E). Both treatment groups exhibited an increase in the Ki-67 levels in the NK cells (figure 4F).

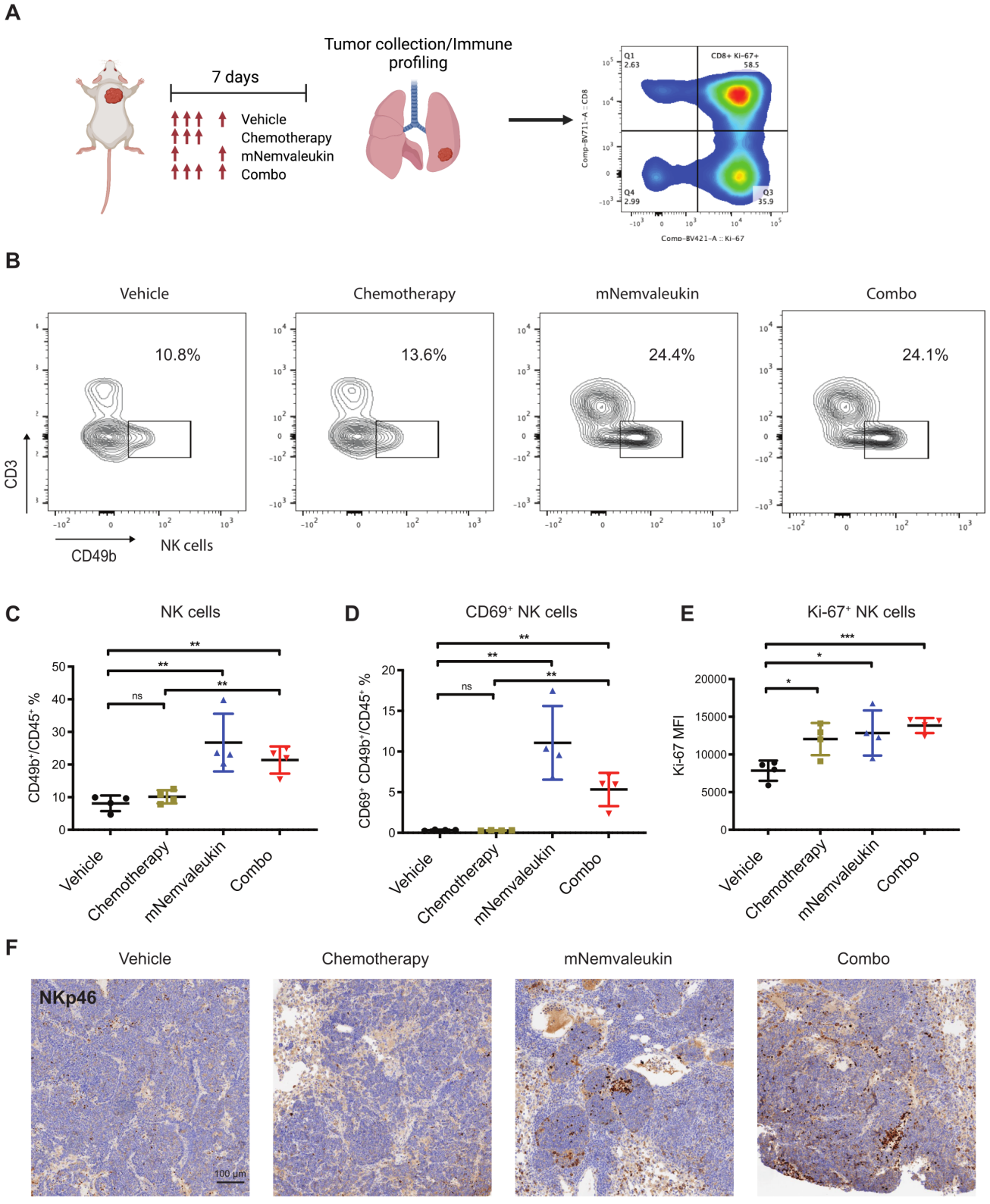


**Figure 2** mNemvaleukin alone and combination treatments expand tumor-infiltrating NK cells in SCLC. (A) Schematic showing experimental design for immune profiling. After confirming tumor burden by MRI, mice were randomized into vehicle, chemotherapy, mNemvaleukin, and combo (chemotherapy+mNemvaleukin) treatment groups. Tumor nodules were collected and tumor-infiltrating lymphocytes were analyzed by flow cytometry at day 7 after treatment initiation. (B) Representative plots of infiltrating NK cells ($CD3^-CD49b^+$) are shown on indicated treatment. (C,D) Frequencies of total infiltrating NK cells (C), activated NK cells (D) and expression of Ki-$67^+$ (E) in NK cells are presented. Two independent cohorts were performed (n=4 in total for each group). (F) IHC staining of NKp46 on tumor samples treated with vehicle, chemotherapy, mNemvaleukin, and combo regimens. Data shown as means±SEM. *P<0.05, **P<0.01, ***P<0.001. IHC, Immunohistochemistry; mNemvaleukin, mouse version of nemvaleukin; NK, natural killer; ns, not significant (unpaired two-tailed t test); SCLC, small cell lung cancer.

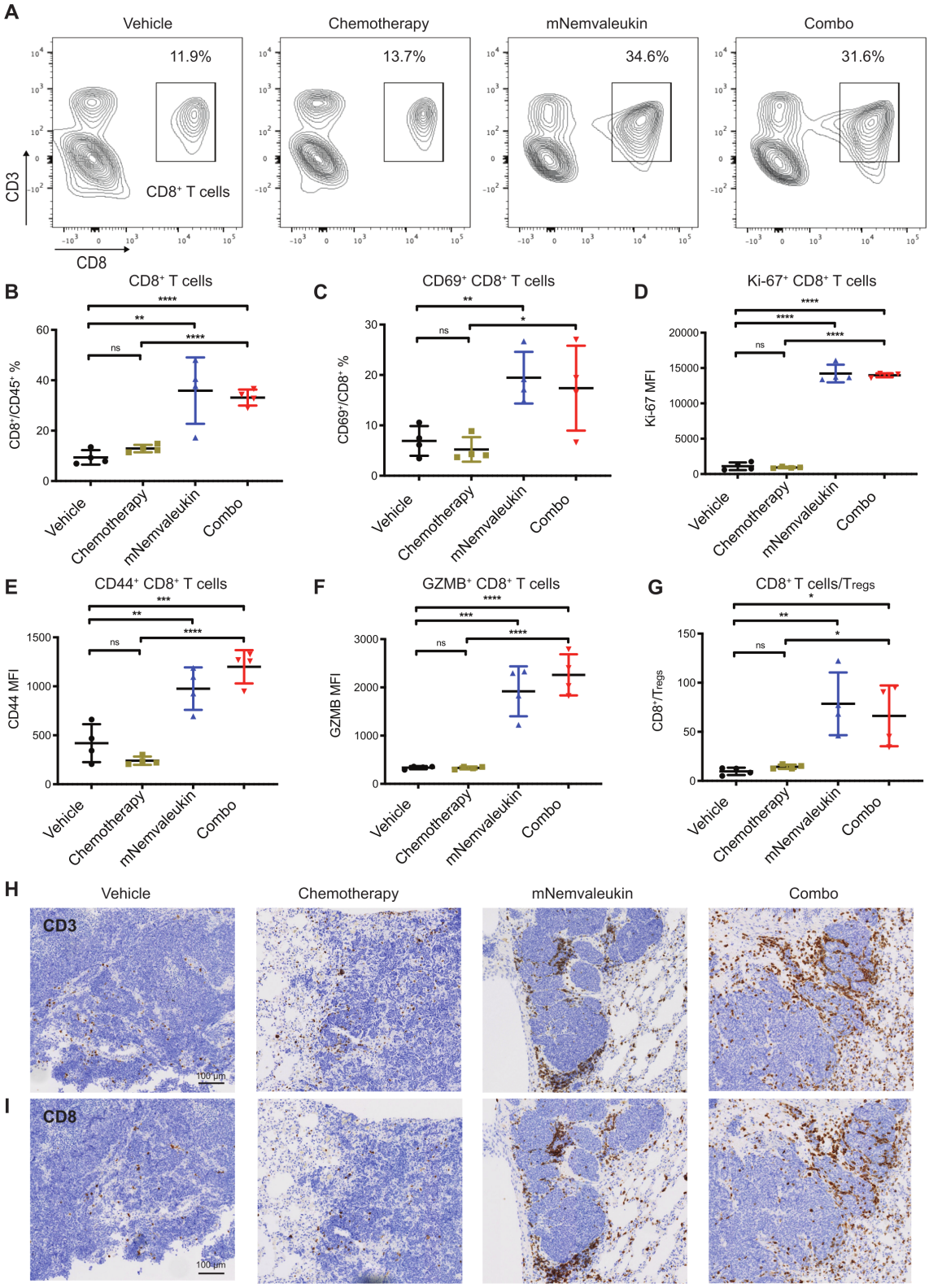


**Figure 3** mNemvaleukin alone and combination treatments expand tumor-infiltrating effector and cytotoxic CD8$^+$ T cells in SCLC. (A) Representative plots of tumor-infiltrating CD8$^+$ T cells (CD3$^+$CD8$^+$) are shown on indicated treatment. (B,C) Frequencies of total infiltrating CD8$^+$ T cells (B), activated CD8$^+$ T cells (C), and expression (median fluorescence intensity, MFI) of Ki-67$^+$ in CD8$^+$ T cells (D) are presented. Expressions of Ki-67$^+$ (D), CD44$^+$ (E), and GZMB$^+$ (F) in CD8$^+$ T cells are presented. (G) The ratios of CD8$^+$ T cells to $T_{regs}$ were analyzed and presented. (H,I) IHC staining of CD3 (H) and CD8 (I) on tumor samples treated with vehicle, chemotherapy, mNemvaleukin and combo regimens. Two independent cohorts were performed (n=4 in total for each group). Data shown as means±SEM. *P<0.05, **P<0.01, ***P<0.001, ****P<0.0001. GZMB, granzyme B; mNemvaleukin, mouse version of nemvaleukin; ns, not significant (unpaired two-tailed t test); SCLC Small cell lung cancer; $T_{reg}$, regulatory T cell.

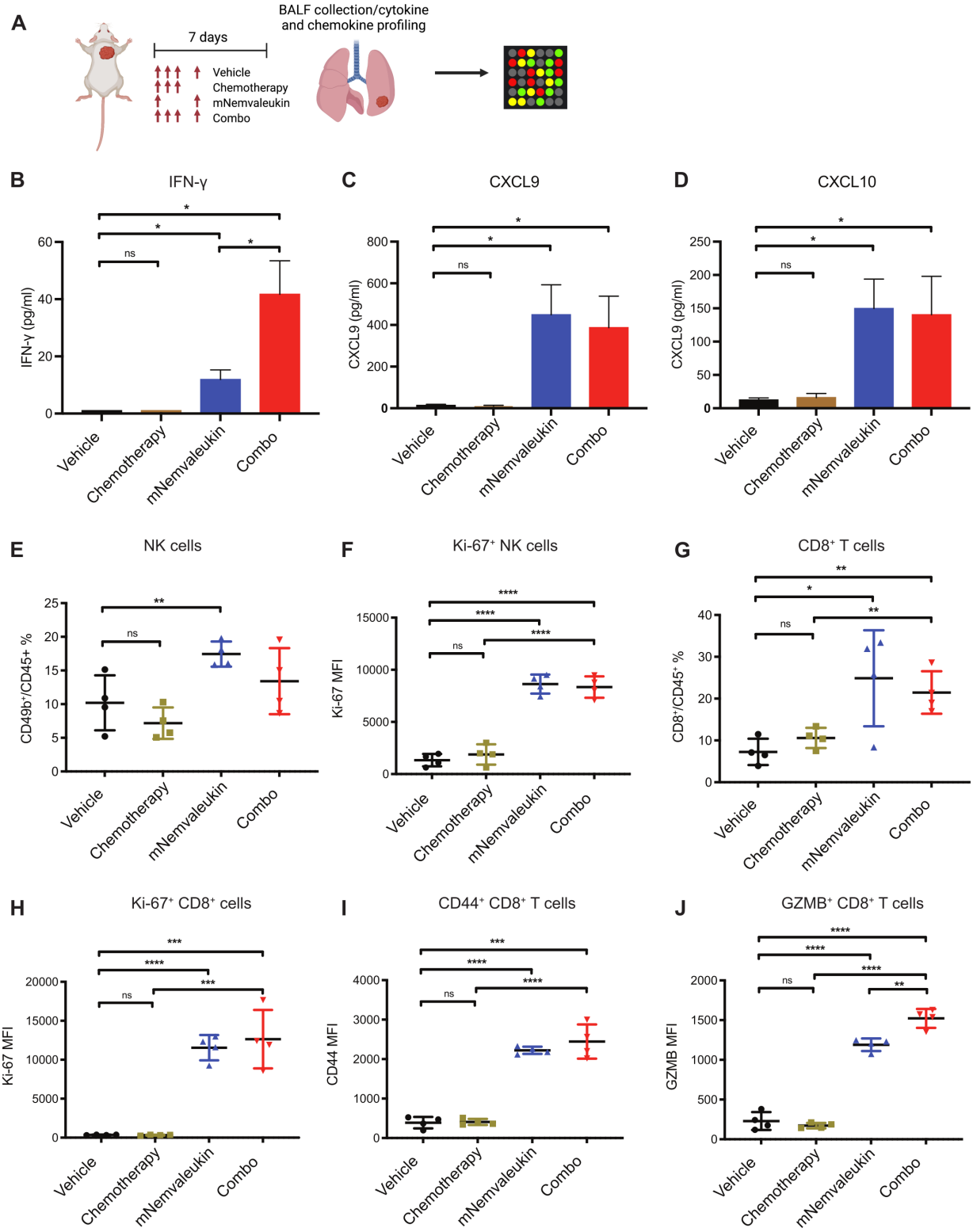


**Figure 4** mNemvaleukin increases proinflammatory cytokines and chemokines and expands activated NK cells and CD8$^+$ T cells in the peripheral blood. (A) Schematic showing experimental design for cytokine and chemokine profiling. After confirming tumor burden by MRI, mice were randomized into vehicle, chemotherapy, mNemvaleukin, and combo treatment groups. BALF was collected from mouse lung and subjected to Luminex analysis. (B–D) Secretions of IFN-γ (B), CXCL9 (C), and CXCL10 (D) were analyzed at day 7 after treatment. (E,F) Frequencies of total NK cells (E) and expression of Ki-67$^+$ in NK cells (F) in the peripheral blood from indicated treatment were analyzed and shown. (G) Frequencies of total CD8$^+$ T cells in peripheral blood were analyzed. (H–J) Expressions of Ki-67$^+$ (H), CD44$^+$ (I) and GZMB$^+$ (J) in CD8$^+$ T cells in the peripheral blood are presented. Two independent cohorts were performed (n=4 in total for each group). Data shown as means±SEM. *P<0.05, **P<0.01, ***P<0.001, ****P<0.0001. BALF, bronchoalveolar lavage fluid; GZMB, granzyme B; IFN-γ, interferon gamma; mNemvaleukin, mouse version of nemvaleukin; NK, natural killer; ns, not significant (unpaired two-tailed t test).

Furthermore, a significant increase of total CD8+ T cells, as well as elevated expression of Ki-67 and CD44 in CD8+ T cells, was detected following mNemvaleukin alone and combination treatments (figure 4G–I). Of note, mNemvaleukin and the combination treatments both dramatically elevated the expression of GZMB in CD8+ T cells in the peripheral blood, with the strongest effect seen in the combination group (figure 4J), further supporting its superior efficacy.

In summary, mNemvaleukin alone and in combination with chemotherapy, significantly promoted proinflammatory cytokines and chemokines production in the TME and expanded activated NK cells and CD8+ T cells in the peripheral blood. The stimulatory effect on cytotoxic CD8+ T cells was further enhanced by the addition of chemotherapy.

### Transcriptomic analysis reveals mNemvaleukin triggers immune response signaling, which is further enhanced by the addition of chemotherapy in SCLC

To comprehensively explore how mNemvaleukin affects immune response signaling in vivo, we performed transcriptomic analysis on tumor nodules after 7 days of treatment. Strikingly, GSEA of the differentially expressed genes revealed the top positively regulated 'immunological signature gene sets' signatures were 'NK-cell activation', 'T-cell activation', and 'CD8+ effector T-cell activation' (figure 5A–F). Heatmaps for the most differentially regulated genes in these top signatures induced by mNemvaleukin showed increased expression of numerous granzyme subfamily members, including *Gmza*, *Gzmb*, *Gzmc*, *Gzmd*, as well as *Prf1* and *Ifng*, which are essential factors involved in NK-cell and CD8+ T-cell killing (figure 5D–F). Moreover, GSEA of the differentially expressed genes showed that the top positively regulated 'hallmark' signatures were also significantly associated with immune response signaling such as 'allograft rejection' (figure 5G–H). These findings consistently support the immune stimulatory effects by mNemvaleukin on NK cells and CD8+ T cells.

In comparison to mNemvaleukin or chemotherapy alone, the combination treatment led to much stronger effects on genes associated with antitumor immune responses (figure 5I–M). GSEA analysis demonstrated that allograft rejection, 'interferon alpha response', and 'IFN-γ response' signatures were significantly over-represented in the combination treatment group (figure 5I–L and online supplemental figure 3A-F). Furthermore, genes related to antigen presentation (*B2m*), interferon signaling (*Irf4*, *Irf7*, and *Irf8*), cytotoxic granzymes (*Gzma*, *Gzma*, *Gzmc*, *Gzmd*, and *Gzme*), NK cells (*Nkg7* and *Ncr1*), and antitumor cytokines/chemokines (*Tnf*, *Ifng*, *Cxcl9*, and *Cxcl10*) are higher following combination treatment, compared with any single agent (figure 5M).

In summary, gene expression analysis indicated that mNemvaleukin induces a robust immune-stimulatory transcription program potentiating NK-cell activation, CD8+ effector T-cell activation, and a robust immune response. Combining mNemvaleukin with chemotherapy further enhances the transcriptional program driving the observed antitumor immunity.

### Singe-cell transcriptomic analysis reveals mNemvaleukin treatment alone and in combination reprogram the immune landscape in the TME

To systematically explore the immunotherapeutic responses following mNemvaleukin treatment alone and in combination, we performed scRNA-seq analysis on the whole TME of SCLC. We harvested and pooled tumors from two mice in each group after 7-day treatment, collected single suspension cells, and analyzed on the 10× Genomics platform. In total, we obtained single-cell transcriptomes for 11,494 cells in the vehicle group, 13,034 in the chemotherapy group, 10,707 in the mNemvaleukin group, and 13,007 in the combination group. Using UMAP for dimension reduction, we identified nine distinct cell clusters according to the gene expression signatures (figure 6A). By further annotating with canonical cell type markers, we identified tumor cells expressing SCLC lineage marker *Ascl1*, T cells expressing *Cd3e*, NK cells expressing *Ncr1*, B cells expressing *Cd19*, and myeloid populations including monocytes, dendritic cells (DCs), macrophages and neutrophils (figure 6B).

To characterize the immune landscape alterations following treatment, we first analyzed the total immune cell proportions in each group. Notably, in comparison to the vehicle, mNemvaleukin treatment increased the frequency of total immune cell populations, which is greatly enhanced by the addition of chemotherapy (figure 6C). Chemotherapy also moderately increased the immune cell frequency, although to a lesser extent. We next compared the immune cell subpopulations of vehicle group with other treatment groups. Remarkably, there is a substantial increase in NK cells and T cells following mNemvaleukin treatment (figure 6D). Combining mNemvaleukin with chemotherapy led to the highest percentage of NK cells and T cells in the TME compared with the other groups. Interestingly, however, mNemvaleukin treatment alone and combination decreased B cells and myeloid populations, including macrophages, monocytes and neutrophils, compared with the vehicle control.

Nemvaleukin is an engineered IL-2 cytokine that selectively activates effector lymphocytes.[25] In line with this, our in vivo immune profiling analysis suggested that mNemvaleukin treatment expanded the cytotoxic NK cells and CD8+ T cells in the TME and peripheral blood. To comprehensively dissect the NK-cell and T-cell subpopulations induced by mNemvaleukin, we further analyzed the scRNA-seq dataset and performed unbiased clustering of the NK and T cells. This approach identified 10 distinct clusters defined by expression of maker genes, suggesting highly heterogenous and complex populations (figure 6E). NK cells represented the most cytotoxic cluster of cells, demonstrated by the highest expression of *Ifng*, *Gzma*, and *Gzmb* (figure 6F). In comparison with the

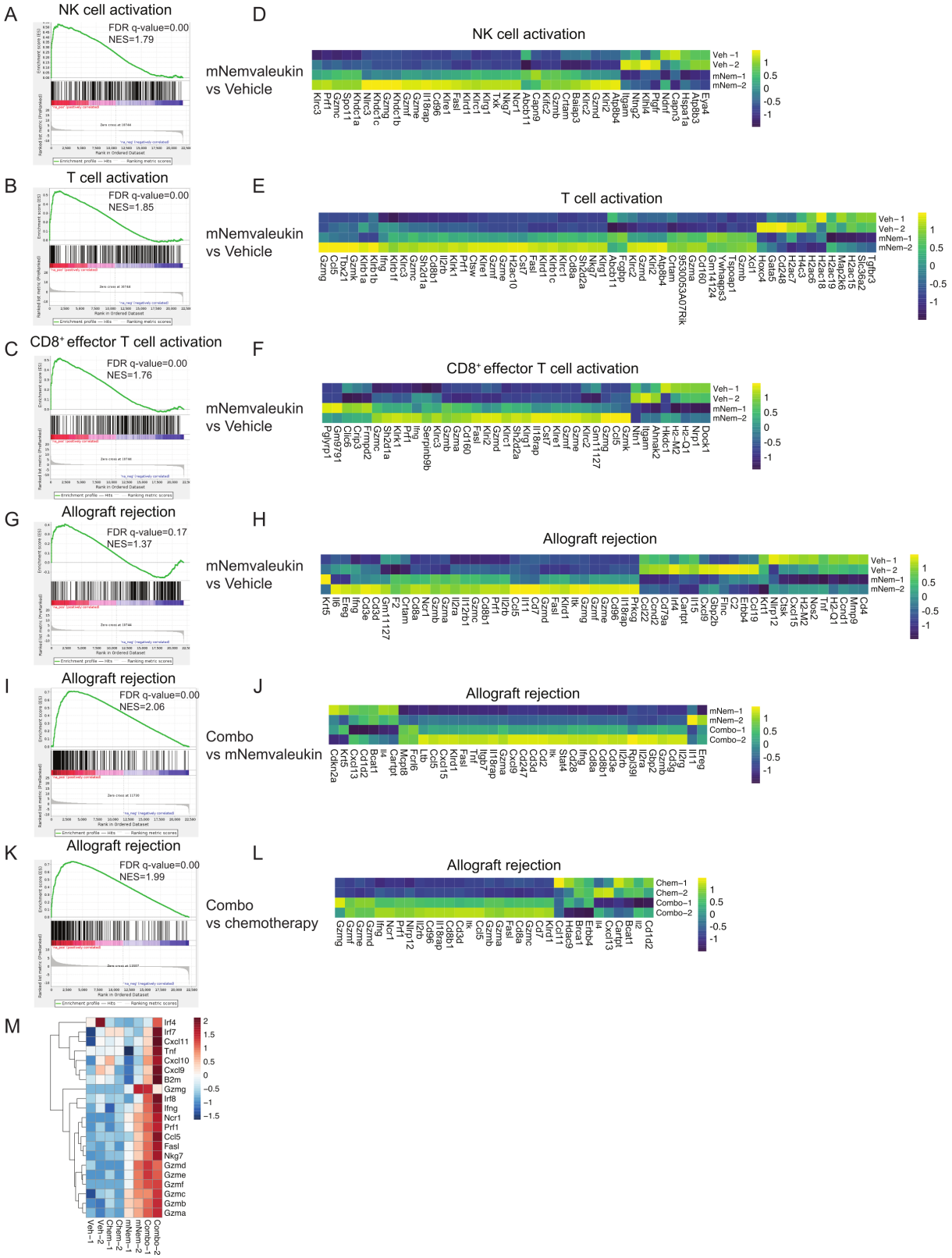


**Figure 5** Transcriptomic analysis reveals mNemvaleukin triggers immune response signaling, which is further enhanced by the addition of chemotherapy in SCLC. (A–H) GSEA and heatmaps of the differentially expressed genes induced by mNemvaleukin, compared with vehicle. Shown are the top positively regulated 'immunological signature gene sets' signatures and 'hallmark' signature. (I–L) GSEA and heatmaps of the differentially expressed genes induced by combo, compared with mNemvaleukin alone (I,J) or chemotherapy (K,L). Shown are the top positively regulated hallmark signature pathways. (M) Heatmap of the differentially expressed genes related to antitumor immunity in vehicle, chemotherapy, mNemvaleukin, and combo groups, respectively. GSEA, gene set enrichment analysis; mNemvaleukin, mouse version of nemvaleukin; NK, natural killer; SCLC, small cell lung cancer.

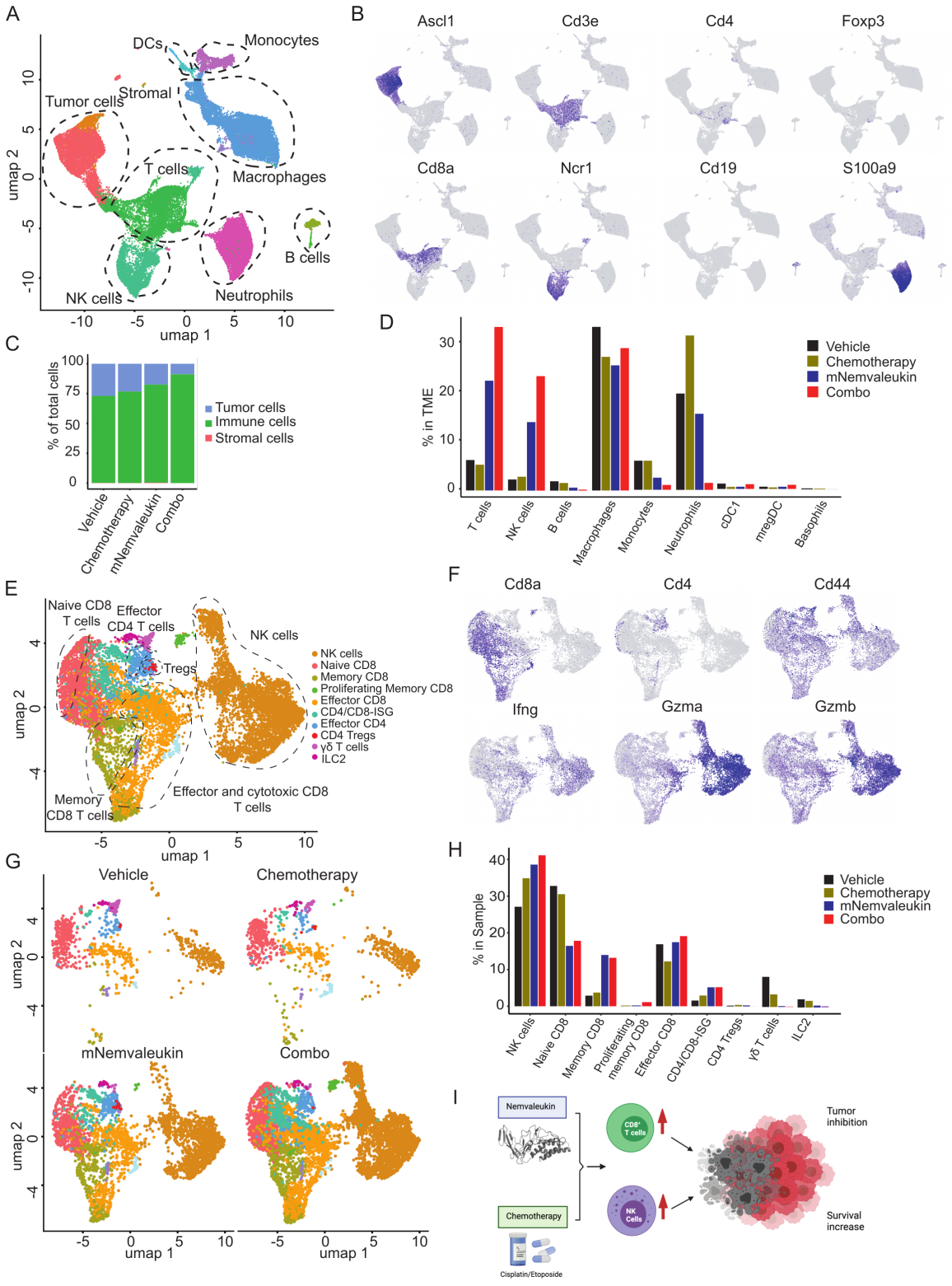


**Figure 6** Single-cell RNAseq analysis of intratumoral immune cell populations demonstrates mNemvaleukin treatment alone and in combination promotes antitumor immunity in the TME. (A) UMAP plot showing identified cell populations including tumor cells, immune cells, and stromal cells. (B) UMAP plots show the expression of cell-type marker genes. (C) Distribution of tumor cells, immune cells, and stromal cells, in response to indicated treatments. (D) Percentage of cells in TME of annotated clusters in response to indicated treatments. (E) UMAP plot showing identified cell subsets in NK and T-cell populations. (F) UMAP plots show the expression selected marker genes. (G) UMAP plots showing distribution of annotated clusters in (E) in response to treatments. (H) Percentage of cells in NK-cell and T-cell populations of annotated clusters in response to indicated treatments. (I) Schematic illustration of the proposed mechanism by combining mNemvaleukin with chemotherapy in SCLC. DC, dendritic cell; NK, natural killer cell; SCLC, small cell lung cancer; TME, tumor microenvironment; UMAP, uniform manifold approximation and projection.

vehicle group, the mNemvaleukin treatment substantially increased the percentage of NK cells, and the combination led to the greatest expansion of NK cells among all groups (figure 6G,H). Interestingly, a slight increase in the frequency of NK cells was also observed after chemotherapy (figure 6G,H).

In the $CD8^+$ T-cell populations, cells with a high level of *Sell* and low levels of *Cd44*, *Ifng*, and *Gzmb* are consistent with naïve and inactivated states and were thus classified as a 'naïve CD8' cluster (figure 6E,F). mNemvaleukin alone and combination treatments markedly reduced the naïve CD8 populations (figure 6G,H). We identified memory $CD8^+$ T cells with high level of memory markers, such as *Eomes,* and intermediate expression of *Gzma* and *Gzmb*. In comparison to the vehicle control, mNemvaleukin and combination treatments led to a pronounced increase in the frequency of memory $CD8^+$ T cells. Furthermore, a cluster of $CD8^+$ T cells shared a similar gene signature with memory T cells but expressed a higher level of the proliferation marker Ki-67 (*Mki67*), which was thus classified as proliferative memory $CD8^+$ T cells. Of note, there were no proliferative memory $CD8^+$ T cells detected in the vehicle group. In comparison to chemotherapy and mNemvaleukin alone groups, combination treatment dramatically expanded the proliferating memory $CD8^+$ T cells (figure 6G,H). Cells in clusters with high *Ifng*, *Gzma*, and *Gzmb* resemble cytotoxic T cells and were classified as 'effector and cytotoxic CD8 T cells'. mNemvaleukin treatment caused an increase in the effector and cytotoxic $CD8^+$ T cells, which is further enhanced by the addition of chemotherapy (figure 6G,H). Moreover, our unbiased clustering also identified $CD4^+$ $T_{regs}$, which express high levels of *Foxp3*. Consistent with our previous observation,[27] $T_{regs}$ accounted for a very small percentage of total immune cell population in the TME of SCLC (< 0.3% of total immune cells). Compared with the vehicle group (0.22%), mNemvaleukin alone slightly increased the $T_{regs}$ proportion (0.28%), but the combo group greatly decreased the percentage of $T_{regs}$ (0.01%).

Collectively, our scRNA-seq analysis reveals a robust antitumor immune response reprogramming in the TME following mNemvaleukin treatment, which is further enhanced by the addition of chemotherapy. These alterations include (1) greatly expanding total NK cells and T cells, (2) reducing the naïve $CD8^+$ T cells, (3) promoting the memory and proliferative memory $CD8^+$ T cells, and (4) increasing the effector $CD8^+$ T cells. Importantly, combining mNemvaleukin with chemotherapy had the most significant increase in expansion of NK cells, proliferative memory, and effector $CD8^+$ T cells.

In conclusion, our immune profiling and comprehensive transcriptomic analysis highlight the immune stimulatory alterations occurring in the TME on mNemvaleukin treatment, and particularly in the combinational therapy. These data further support the beneficial effects of mNemvaleukin alone and in combination with chemotherapy on the antitumor response and survival (figure 6I).

## DISCUSSION

SCLC is a recalcitrant disease with a 5-year relative survival rate of less than 7% and the loss of approximately 30-000 lives per year in the USA. Treatment regimens in SCLC remain largely unchanged in the past few decades. The Food and Drug Administration recently approved the addition of immunotherapy (such as anti-PD-L1) to chemotherapy for the first-line treatment of adult patients with ES-SCLC.[13] However, the added benefit to median OS was only approximately 2 months, highlighting an urgent need to develop new therapeutic strategies for patients with SCLC.

In this work, we demonstrate that mNemvaleukin, a fusion protein of circularly permuted IL-2 to the extracellular domain of IL-2Rα, inhibits tumor growth and improves survival in SCLC, wherein it drives a strong antitumor immunity program through expansion of activated NK and $CD8^+$ T cells. Combining mNemvaleukin with chemotherapy leads to a more robust immune response and confers remarkable survival benefit in this highly aggressive cancer. Our findings provide a rationale for combining nemvaleukin and chemotherapy for patients with SCLC.

Despite the association with high TMBs, patients with SCLC showed an extremely low overall response rates to ICBs, which could partly be due to (1) low or absent PD-L1 expression, (2) low human leukocyte antigen (HLA) expression, or (3) poor immune cell infiltration. Indeed, the TME of SCLC features decreased immune cell infiltration defined as a cold or 'immune desert' phenotype, based on low levels of immune cell-related RNA expression. Further IHC staining of tissue from patients with SCLC also supported an immune desert phenotype, associated with low numbers of tumor infiltrating lymphocytes including $CD45^+$, $CD3^+$, $CD8^+$, and $CD20^+$ cells.[15 16] To address this challenge, several elegant studies have recently explored novel approaches to enhance immune cell infiltration and target cytotoxic effector populations. Best and colleagues demonstrated that harnessing the cytotoxic capacity of NK cells by modulating IL-15 and transforming growth factor beta (TGF-β) signaling was efficacious in restricting the dissemination of SCLC.[17] Likewise, Zhu and colleagues revealed a lack of surface ligands for NK-activating receptor NKG2D in both preclinical and clinical samples of SCLC, indicating an impairment of an inherent mechanism of tumor cell recognition by the innate immune system. Restoring NKG2DL expression through pan-HDAC (histone deacetylases) inhibitors triggered antitumor immunity by recruiting and activating NK cells and T cells in preclinical models.[18] These encouraging data strongly support further exploration of alternative targets to enhance the activation of cytotoxic effector populations in SCLC.

IL-2 was the first effective immunotherapy for human cancer shown to induce durable responses in a subset of patients with metastatic melanoma and renal cell carcinoma.[22] However, the use of natural IL-2 for cancer treatment has been significantly compromised by its

double-edged activity. Due to a better understanding of IL-2/IL-2R structure/biology and the improvement of protein engineering technology, multiple engineered IL-2 moieties designed to achieve better selectivity and reduced toxicity are in preclinical and clinical development.[33–37] However, the effects of engineered IL-2 variants have not been extensively evaluated in SCLC. Previous work demonstrated that nemvaleukin is a novel circularly permuted IL-2-IL2Rα fusion protein that preferentially activates and expands NK cells and effector $CD8^+$ T cells.[25 38] Here, we explored the in vivo therapeutic potential of combining mNemvaleukin with chemotherapy in a novel murine model with lung TME to closely model human disease. Of note, mNemvaleukin inhibits SCLC tumor growth and enhances tumor response to chemotherapy. Combining mNemvaleukin with chemotherapy significantly extends OS in an SCLC preclinical model, supporting the potential of mNemvaleukin in enhancing immunity as a backbone for combinational treatment.

Our mechanistic studies to examine the TME alterations uncovered that mNemvaleukin alone and in combination with chemotherapy dramatically expand tumor-infiltrating NK cells and effector $CD8^+$ T cells, which are highly active and proliferating. In particular, a highly cytotoxic $GZMB^+CD8^+$ T-cell population and a significantly higher $CD8^+/T_{regs}$ ratio were observed on treatment with mNemvaleukin alone and in combination. Further characterization of factors that are responsible for antitumor immune responses by Luminex and transcriptomic analysis showed a pronounced secretion of proinflammatory cytokines and chemokines such as IFN-γ, CXCL9, and CXCL10. Intriguingly, combining mNemvaleukin with chemotherapy had the most immunostimulatory effects in driving the immune surveillance program elicited by NK and T cells in SCLC.

Furthermore, our comprehensive scRNA-seq analysis supports a strong antitumor immune program elicited by cytotoxic immune cells in the TME on mNemvaleukin alone and in combination. Our analysis uncovered several key features and alterations on immune compartments: mNemvaleukin (1) dramatically expanded the NK-cell and T-cell populations, (2) caused a significant shift from naïve $CD8^+$ T cells to effector $CD8^+$ T cells, (3) promoted the growth of the memory and proliferative memory $CD8^+$ T cells. Importantly, our scRNA-seq analysis further highlights that combining mNemvaleukin with chemotherapy led to the most significant increase in expansion of NK cells, proliferative memory, and effector $CD8^+$ T cells, potentiating its superior antitumor immunity in SCLC. Further detailed mechanistic studies on the synergy of antitumor immunity by combining mNemvaleukin and chemotherapy are warranted in the future.

In line with recent work,[17 18] our study highlights the therapeutic potential of enhancing NK-cell and T-cell activity through IL-2 signaling as a new approach in SCLC. Our work supports the combination approach of nemvaleukin and chemotherapy in future SCLC clinical trials. Considering the broad effects of the IL-2 signaling pathway in driving immune responses, combining nemvaleukin with existing standard-of-care therapies including chemotherapy might prove to be a widely applicable new approach in cancer treatment, particularly in immune desert subtypes.

**Author affiliations**
[1]Laura and Isaac Perlmutter Cancer Center, NYU Langone Health, New York, New York, USA
[2]Applied Bioinformatics Laboratories, Office of Science and Research, New York University Grossman School of Medicine, New York, New York, USA
[3]Research, Alkermes Inc, Waltham, Massachusetts, USA

**Acknowledgements** The authors thank Alkermes for funding support and also the members of the Wong laborartory for their experimental support and insightful discussion.

**Contributors** Designing of research studies: HZ, YP, HCL, JEL, RJW, VV, and KKW; conducting experiments: YP, HZ, HH, TC, HD, KEL, ES, KG, HH, FS, KG, JS, AC, ST, HYH, and CP; data analysis: YP, YH and HZ; writing of the manuscript: HZ and YP. All authors read and approved the final manuscript. YP, HZ and KKW are the guarantors of this study.

**Funding** These studies were funded by Alkermes, Waltham, Massachusetts.

**Competing interests** HCL, JEL, and RJW are current employees of and hold stock in Alkermes. Research performed at New York University Grossman School of Medicine in the laboratory of KKW was funded by Alkermes. KKW is a founder and equity holder of G1 Therapeutics and has sponsored research agreements with MedImmune, Takeda, TargImmune, Bristol-Myers Squibb (BMS), Mirati, Merus, and Alkermes, and consulting and sponsored research agreements with AstraZeneca, Janssen, Pfizer, Novartis, Merck, Ono, and Array. VV has advisory/consult role at Genentech, Merck, BMS, AstraZeneca, Foundation Medicine, Nektar Therapeutics, Alkermes, Reddy labs, and Millennium Pharma.

**Patient consent for publication** Not applicable.

**Ethics approval** All animal studies were reviewed and approved by the Institutional Animal Care and Use Committee at the New York University Langone Health.

**Provenance and peer review** Not commissioned; externally peer reviewed.

**Data availability statement** Data are available in a public, open access repository.



**ORCID iD**
Hua Zhang http://orcid.org/0000-0001-7704-4712

## REFERENCES

1 van Meerbeeck JP, Fennell DA, De Ruysscher DKM. Small-Cell lung cancer. *Lancet* 2011;378:1741–55.
2 Rudin CM, Brambilla E, Faivre-Finn C, *et al*. Small-Cell lung cancer. *Nat Rev Dis Primers* 2021;7:3.
3 Bunn PA, Minna JD, Augustyn A, *et al*. Small cell lung cancer: can recent advances in biology and molecular biology be translated into improved outcomes? *J Thorac Oncol* 2016;11:453–74.

4 Semenova EA, Nagel R, Berns A. Origins, genetic landscape, and emerging therapies of small cell lung cancer. *Genes Dev* 2015;29:1447–62.
5 Alexandrov LB, Nik-Zainal S, Wedge DC, *et al*. Signatures of mutational processes in human cancer. *Nature* 2013;500:415–21.
6 George J, Lim JS, Jang SJ, *et al*. Comprehensive genomic profiles of small cell lung cancer. *Nature* 2015;524:47–53.
7 Peifer M, Fernández-Cuesta L, Sos ML, *et al*. Integrative genome analyses identify key somatic driver mutations of small-cell lung cancer. *Nat Genet* 2012;44:1104–10. ng.2396 [pii].
8 Rudin CM, Durinck S, Stawiski EW, *et al*. Comprehensive genomic analysis identifies Sox2 as a frequently amplified gene in small-cell lung cancer. *Nat Genet* 2012;44:1111–6.
9 Bagchi S, Yuan R, Engleman EG. Immune checkpoint inhibitors for the treatment of cancer: clinical impact and mechanisms of response and resistance. *Annu Rev Pathol* 2021;16:223–49.
10 Alexandrov LB, Nik-Zainal S, Wedge DC, *et al*. Signatures of mutational processes in human cancer. *Nature* 2013;500:415–21.
11 Hellmann MD, Callahan MK, Awad MM, *et al*. Tumor mutational burden and efficacy of nivolumab monotherapy and in combination with ipilimumab in small-cell lung cancer. *Cancer Cell* 2018;33:853–61.
12 Iams WT, Porter J, Horn L. Immunotherapeutic approaches for small-cell lung cancer. *Nat Rev Clin Oncol* 2020;17:300–12.
13 Horn L, Mansfield AS, Szczęsna A, *et al*. First-Line Atezolizumab plus chemotherapy in extensive-stage small-cell lung cancer. *N Engl J Med* 2018;379:2220–9.
14 Paz-Ares L, Dvorkin M, Chen Y, *et al*. Durvalumab plus platinum-etoposide versus platinum-etoposide in first-line treatment of extensive-stage small-cell lung cancer (Caspian): a randomised, controlled, open-label, phase 3 trial. *Lancet* 2019;394:1929–39.
15 Carvajal-Hausdorf D, Altan M, Velcheti V, *et al*. Expression and clinical significance of PD-L1, B7-H3, B7-H4 and TILs in human small cell lung cancer (SCLC). *J Immunother Cancer* 2019;7:65.
16 Dora D, Rivard C, Yu H, *et al*. Neuroendocrine subtypes of small cell lung cancer differ in terms of immune microenvironment and checkpoint molecule distribution. *Mol Oncol* 2020;14:1947–65.
17 Best SA, Hess JB, Souza-Fonseca-Guimaraes F, *et al*. Harnessing natural killer immunity in metastatic SCLC. *J Thorac Oncol* 2020;15:1507–21.
18 Zhu M, Huang Y, Bender ME, *et al*. Evasion of innate immunity contributes to small cell lung cancer progression and metastasis. *Cancer Res* 2021;81:1813–26.
19 Ross SH, Cantrell DA. Signaling and function of interleukin-2 in T lymphocytes. *Annu Rev Immunol* 2018;36:411–33.
20 Liao W, Lin J-X, Leonard WJ. Interleukin-2 at the crossroads of effector responses, tolerance, and immunotherapy. *Immunity* 2013;38:13–25.
21 Rosenberg SA, Yang JC, White DE, *et al*. Durability of complete responses in patients with metastatic cancer treated with high-dose interleukin-2: identification of the antigens mediating response. *Ann Surg* 1998;228:307–19.
22 Rosenberg SA. Il-2: the first effective immunotherapy for human cancer. *J Immunol* 2014;192:5451–8.
23 Payne R, Glenn L, Hoen H, *et al*. Durable responses and reversible toxicity of high-dose interleukin-2 treatment of melanoma and renal cancer in a community hospital biotherapy program. *J Immunother Cancer* 2014;2:13.
24 Malek TR, Bayer AL. Tolerance, not immunity, crucially depends on IL-2. *Nat Rev Immunol* 2004;4:665–74.
25 Lopes JE, Fisher JL, Flick HL, *et al*. ALKS 4230: a novel engineered IL-2 fusion protein with an improved cellular selectivity profile for cancer immunotherapy. *J Immunother Cancer* 2020;8:e000673.
26 Lopes JE, Sun L, Flick HL. Pharmacokinetics and pharmacodynamic effects of Nemvaleukin alfa, a selective agonist of the Intermediate-Affinity IL-2 receptor, in cynomolgus monkeys. *J Pharmacol Exp Ther* 2021 (published Online First: 2021/08/08).
27 Zhang H, Christensen CL, Dries R, *et al*. Cdk7 inhibition potentiates genome instability triggering anti-tumor immunity in small cell lung cancer. *Cancer Cell* 2020;37:37–54.
28 Dobin A, Davis CA, Schlesinger F, *et al*. Star: ultrafast universal RNA-seq aligner. *Bioinformatics* 2013;29:15–21.
29 Li B, Dewey CN. RSEM: accurate transcript quantification from RNA-Seq data with or without a reference genome. *BMC Bioinformatics* 2011;12:323.
30 Subramanian A, Tamayo P, Mootha VK, *et al*. Gene set enrichment analysis: a knowledge-based approach for interpreting genome-wide expression profiles. *Proc Natl Acad Sci U S A* 2005;102:15545–50.
31 Liberzon A, Subramanian A, Pinchback R, *et al*. Molecular signatures database (MSigDB) 3.0. *Bioinformatics* 2011;27:1739–40.
32 Butler A, Hoffman P, Smibert P, *et al*. Integrating single-cell transcriptomic data across different conditions, technologies, and species. *Nat Biotechnol* 2018;36:411–20.
33 Mullard A. Restoring IL-2 to its cancer immunotherapy glory. *Nat Rev Drug Discov* 2021;20:163–5.
34 Diab A, Tykodi SS, Daniels GA, *et al*. Bempegaldesleukin plus nivolumab in first-line metastatic melanoma. *J Clin Oncol* 2021;39:2914–25.
35 Ptacin JL, Caffaro CE, Ma L, *et al*. An engineered IL-2 reprogrammed for anti-tumor therapy using a semi-synthetic organism. *Nat Commun* 2021;12:4785.
36 Silva D-A, Yu S, Ulge UY, *et al*. De novo design of potent and selective mimics of IL-2 and IL-15. *Nature* 2019;565:186–91.
37 Hsu EJ, Cao X, Moon B, *et al*. A cytokine receptor-masked IL2 prodrug selectively activates tumor-infiltrating lymphocytes for potent antitumor therapy. *Nat Commun* 2021;12:2768.
38 Lopes JE, Sun L, Flick HL, *et al*. Pharmacokinetics and pharmacodynamic effects of Nemvaleukin alfa, a selective agonist of the Intermediate-Affinity IL-2 receptor, in cynomolgus monkeys. *J Pharmacol Exp Ther* 2021;379:203–10.